

TADEUSZ CZECH\* ,ANDRZEJ KRUPA\*, MARCIN LACKOWSKI\*, ERYK RAJCH\*\*

## DUST COMPONENTS IDENTIFICATION BY EMISSION SPECTROSCOPY IN BACK DISCHARGE

The results of emission spectroscopic analysis of back discharge generated in the point-to-plane electrode covered with fly ash layer of high resistivity in ambient air were presented. The visual forms of the discharge were recorded with digital camera referred to the current–voltage characteristics and optical emission spectra. The interest in these studies was motivated by detrimental effects which this type of discharge causes in the electrostatic precipitators. The studies have shown that the spectral lines omitted the back discharge are unique and dependent on discharge current. The spectral lines could be used for investigation of dust layer composition.

### 1. INTRODUCTION

Back discharge is an abnormal discharge caused by a breakdown of high-resistivity layer formed by dust particles deposited on the collection electrode [1]. Farther collection of dust particles becomes difficult when the collection plate is covered with a layer of particles of high resistivity. It is caused by electric field reduction in the interelectrode space due to the electric charge accumulated at the layer. When the potential at the layer reaches a threshold level, a local breakdown of the layer occurs, which may trigger a discharge within the layer. The discharge in this specified point (even a few points) becomes an ions source. The ions of polarity as the discharge electrode flow through the layer to the collection electrode while those of opposite polarity are emitted into the interelectrode space. These ions can be deposited on the dust particles, reducing their charge and decreasing the collection efficiency [2]. The purpose of this paper is to propose an application of powerful tool such as optical emission spectroscopy in back discharge studies. The technique is capable of detecting elements at sub-ppb level with good accuracy and precision. The emitted light can be analysed by optical emission spectroscopy and provides information on the type of this discharge and relative concentration of ex-

---

\* Institute of Fluid Flow Machinery, PAN, 80-952 Gdańsk, Fiszerka 14, Poland.

\*\* Institute of Physics, Pomeranian Pedagogical Academy, 76-200 Słupsk, Arciszewskiego 22, Poland.

ited species present in the discharge space in the case of back-discharge, also on the elements emitted from the dust layer. In the present paper, the current-voltage characteristics of the back discharge, visual forms of various types of back discharges and spectroscopic analysis of ionization and excitation of the molecules are presented. Optical emission spectroscopy is an accurate and non-disturbing plasma diagnostic tool. It allows us to obtain information on vibration and rotational electron states of atoms and molecules. All data on the wavelength of spectral lines necessary for the purpose of this paper were obtained from [3].

## 2. EXPERIMENTAL SET-UP

A schematic diagram of the experimental set-up used is shown in figure 1.

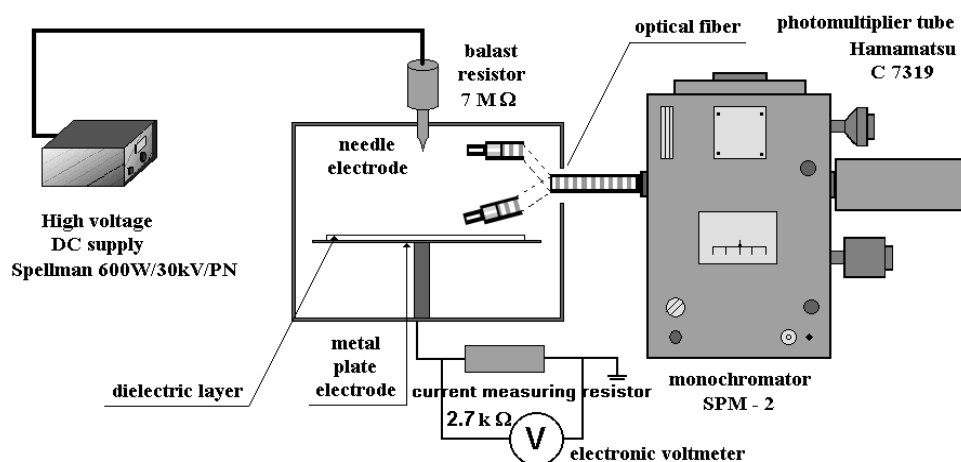


Fig. 1. Schematic diagram of the experimental set-up

The discharge chamber was made of acrylic glass of the following dimensions: 560 mm in length, 100 mm in width and 80 mm in height. The electrodes, a stainless steel needle and a plate, were placed in the middle of the chamber in the half of its length. The discharges were generated in the air at atmospheric pressure and a temperature of 23 °C and 45% relative humidity. The grounded plate was covered with a fly ash layer of the thickness of 5 or 8 mm. The interelectrode gap (the distance between the tip of needle and metal plate) was fixed at 20 mm. A high-voltage dc source HV SL600W/30 kV/PN (Spellman supplied) supplied the electrodes. A ballast resistor of 7 MΩ was connected in series in order to stabilize the discharge current. For the determination of the discharge current a resistor of 2.7 kΩ was used, at which the voltage drop was measured by an electronic voltmeter. The current was calculated from the Ohms law.

The SPM-2 spectrometer (Carl-Zeiss-Jena) was provided with the light from the discharge by optical fiber. The optical fiber was pointed either to the plasma on the fly ash layer or to the tip of needle electrode. The resolution of the spectrometer was about 0.5 nm for the width of the entrance slit of 1–0.4 mm, and a grating of 1300 grooves/mm. A photomultiplier tube R375 (Hamamatsu) and signal preamplifier unit C7319 (Hamamatsu) were used to detect the optical signals. The emission spectrum was measured in the spectral range of 200–600 nm. The discharge was generated in the air flowing perpendicularly to the needle electrode axis. A glass window of 52 mm diameter was used in order to take the photographs of the discharge. The photographs were taken with a digital camera Panasonic NV-GS400 equipped with lens (RAYNOX MACROSCOPIC LENS M-250).

### 3. CURRENT VOLTAGE CHARACTERISTICS

An effect of thickness of dust layer on back discharge was studied using fly ash layer of 5 or 8 mm thickness. The current–voltage characteristics of the discharge are shown in figure 2. The resistivity of the dust was higher than  $10^{14} \Omega/\text{m}$ . From figure 2 it can be seen that with an increase of the layer thickness the voltage for which streamer discharge occurs also increases. However, for lower voltages, no significant effect of the layer thickness on the characteristics has been observed. Figure 3 shows a series of photographs of various forms of back discharge in air with the supply volt-

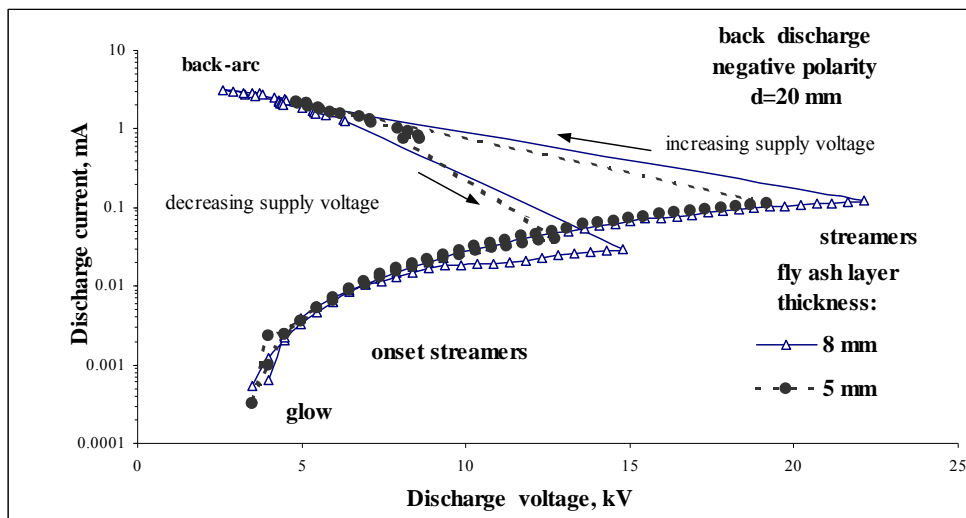


Fig. 2. Current–voltage characteristics of a negative back corona discharge in the air at atmospheric pressure for different fly ash layer thickness

age increasing. The needle electrode is at the top of figure 3, and the grounded plate electrode is beneath. The photographs clearly show all different stages of the back discharge development with an increasing voltage. For lower voltages a glow surrounding the needle can be observed. Similar glow can be noticed in breakdown points on the dust layer surface. If the voltage is sufficiently high, the streamer discharge initiates from the craters on the layer. The streamer expands towards the discharge electrode (needle) bridging the interelectrode space. For the layer thickness of 8 mm, the glow discharge was observed up to 17 kV. Also the back arc started for higher voltage at about 23 kV. This effect can be explained by the higher voltage drop across the layer.

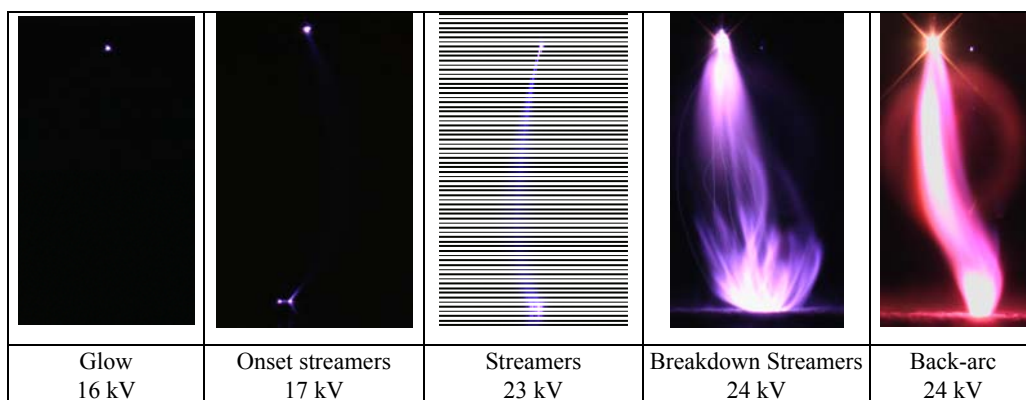


Fig. 3. Forms of back-discharge for different voltages of negative polarity; 5 mm thickness of fly ash layer

#### 4. SPECTROSCOPIC MEASUREMENTS

Electrical discharges produce a transient and weakly ionized plasma heated by electrons and other species (excited atoms, molecules, etc.). Plasma is characterised by different temperatures of these species. Inelastic collisions between electrons and molecules of fly ash lead to very complicated processes: dissociation, recombination, formation of excited fragments, etc. The plasma created by back corona can roughly be divided into two different zones separated by a dark space: *needle tip zone* (being located in the vicinity the needle electrode tip and extending into the inter-electrode space) and *crater zone* (being located close to the craters on the dielectric layer). The size of the zones depends on the power delivered to the discharge. Emission spectra of back discharge were measured in the wavelength range of 200–600 nm. In the case of atmospheric corona and back corona discharges, spectra at the needle tip are dominated by the emission of the second positive system of  $N_2$ . Therefore it can be concluded that dissociation of diatomic species is important for this type of discharges. During the discharge, the creation of NO can be also ob-

served ( $\gamma$ -system). Atomic lines in different intervals of wavelengths with comparable “very weak” intensities can be easily lost in the molecular bands given in the table. The OH lines exceeded the height of the tail of  $N_2$  at 308 nm. The OH band at 306.4 nm appears, particularly when small traces of water vapour are present in the dust layer or air. The molecular spectra observed have very high molecular background.

Table

Identified band wavelengths of the second positive system of  $N_2$   
for the sequence ( $\Delta v = -2; -1; 0; 1; 2$ ) [3]

$\Delta v' = -2$			$\Delta v' = -1$			$\Delta v' = 0$			$\Delta v' = 1$			$\Delta v' = 2$		
$\lambda$ [nm]	$v'$	$v''$	$\lambda$ [nm]	$v'$	$v''$	$\lambda$ [nm]	$N_2$	$v''$	$\lambda$ [nm]	$v'$	$v''$	$\lambda$ [nm]	$v'$	$v''$
380.49	0	2	357.69	0	1	337.13	0	0	315.93	1	0	297.68	2	0
375.54	1	3	353.67	1	2	333.9	1	1	313.60	2	1	296.20	3	1
371.05	2	4	311.62	3	2	328.53	3	3	311.67	3	2	295.32	4	2
367.19	3	5	315.93	1	0				310.40	4	3			
364.17	4	6	346.69	3	4									

Every spectrum contains the sequence ( $\Delta v = -2; -1; 0; 1; 2$ ) of the second positive system of  $N_2$  molecule band which predominates in the spectrum (figures 4–6). These

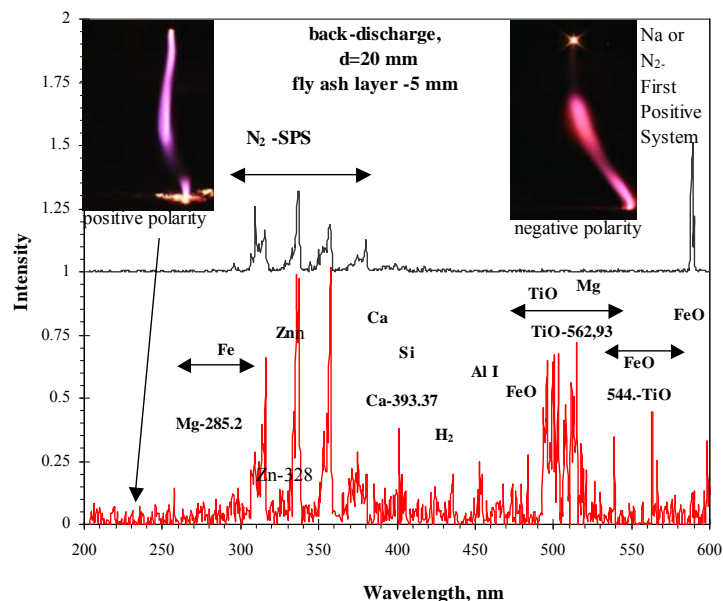


Fig. 4. Comparison of back-corona discharge emission spectra for positive and negative needle polarities in the layer zone. Supply voltage of 20 kV and 24 kV, discharge current of 1.70 mA and 2.78 mA,

respectively. Thickness of fly ash layer of 5 mm

bands originate from molecular dissociation products, being created during plasma discharge. The molecular transitions observed are listed in the table. The intensity ratios of the second positive system of  $N_2$  indicate that peak electron energy approaches 15 eV. This system involves a fully allowed transition, with electronic energy levels above 9.76 eV [3]. The lines of TiO emission ( $\lambda = 562.9$  nm, 544.2 nm) are observed (figure 5) in the needle tip zone, which proves that fine particles from this fly ash are introduced into the plasma and flow to the needle electrode. Finally, weak emission lines of metals (Co, Mo, Fe, Ni) are detected. These lines indicate that

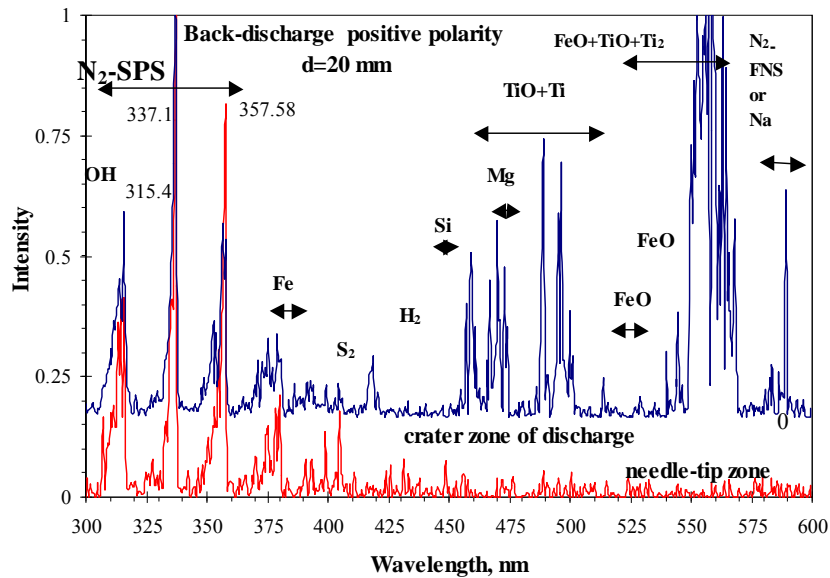


Fig. 5. Spectra of back-arc discharge in different zones. Positive needle polarity (supply voltage of 26 kV). Thickness of fly ash layer of 8 mm

electrons in the gas discharge occurring at the electrode tip excite the atoms of the electrode material. It should be stressed that iron atoms are oxidized during the discharge in the air and the spectrum has very weak FeO band. In the electrode needle-tip zone, there are also some additional atomic lines (Fe- $\lambda = 430.79$  nm, Co- $\lambda = 412.13$  nm, Mo- $\lambda = 379.8$  nm). Discharges are very effective in energy transfer between electrons and atoms and ions by electron collisions. These collisions create metastable states of atoms. Back arc, however, produces many ions from the dust layer. The emission lines of  $Ti_2$  and TiO transitions at 567 nm, 561 nm, 498 nm were apparent in the back arc discharge in the layer zone (figure 7). In order to understand the processes, which are involved in the back corona discharge, spectroscopic measurements

in the crater zone of the discharge for positive and negative polarities are carried out (figure 6). The spectroscopic results suggest that the back corona discharge mechanisms for the same discharge power greatly depend on the polarity of a discharge electrode.

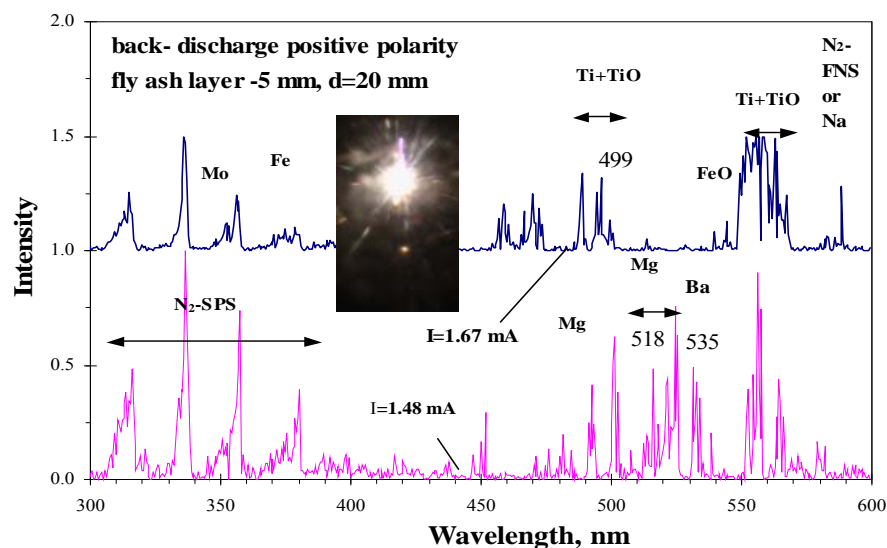


Fig. 6. Spectrum of back discharge of positive polarity in the air at atmospheric pressure for different discharge currents. Supply voltage of 24 kV. Thickness of fly ash layer of 5 mm

As opposed to the above, in positive back corona, the most dominant band is the second positive system of  $N_2$  (the table). The back discharge in the back arc mode bridges the interelectrode gaps, triggering the breakdown due to accumulation of ions on the layer. If the value of the voltage applied was fixed, the current and the intensity of the light emitted by the discharge slowly changed (figure 6).

## 5. CONCLUSIONS

The back discharge plasma has been studied with respect to current–voltage characteristics of the discharge, emission spectra. Molecular species of ambient air have been introduced under experimental conditions into plasma region and the resulting emission has been studied. Emission of the second positive system of  $N_2$  molecules in the discharge have been recognized in the emission spectra. Further, atomic fragments and dissociation products such as OH and NO are present in the spectrum. The OH radicals are formed as a result of the dissociation of  $H_2O$ , which is always present in

trace amount as water vapour in the ambient air. The emission spectra observed in the needle-tip zone have some lines from dust layer elements. This is the consequence of passing the dust particles from the layer to the interelectrode zone (figure 6). In this paper, spectroscopic studies on several back corona plasmas that can occur in electrostatic precipitators have been presented.

#### REFERENCES

- [1] BACH S., *Procesy fizyczne w elektrofiltracji aerozoli*, III Konferencja *Eksploatacja elektrofiltrów w energetyce*, ELEKTROFILTRY'92, 20–21 listopada 1992, Kraków.
- [2] MASUDA S., *Recent progress in electrostatic precipitation*, Static Electrification, 1975, Inst. Phys. Conf. Series No. 27, 154.
- [3] PEARSE R.W.B., GAYDON A.G., *The Identification of Molecular Spectra*, Chapman and Hall, London, 1963.

#### IDENTYFIKACJA ZANIECZYSZCZEŃ PYŁOWYCH PODCZAS WYŁADOWANIA WSTECZNEGO ZA POMOCĄ SPEKTROSKOPII EMISYJNEJ

Wyładowanie wsteczne powstaje na elektrodzie biernej w obecności warstwy dielektrycznej o dużej rezystywności. Przedstawiono wyniki badań wyładowania wstecznego dla elektrody uziemionej, pokrytej warstwą pyłu z elektrofiltru. Strimery w wyładowaniu wstecznym rozwijają się pomiędzy elektrodą ulotową a kraterem powstałym w warstwie dielektrycznej. Gdy zwiększa się napięcie, wyładowanie strimerowe może przejść w wyładowanie łukowe. Cechą wyładowania wstecznego do warstwy pyłu w powietrzu jest pojawienie się intensywnego pasma molekularnego azotu ( $N_2$ ). Oprócz głównych pasm azotu zidentyfikowano również pasma NO i  $NO_2$  o mniejszej intensywności. Obserwowano również linie atomowe pierwiastków, np. Co, Fe, Mo, Ni, Ti, oraz ich tlenków. W wyniku wyładowania metale z pyłu osadzonego na elektrodzie mogą być wtórnie emitowane do atmosfery.